*J. Fluid Mech.* (1987), *vol.* 185, *pp.* 275–288
*Printed in Great Britain*



# Ideal jet flow in two dimensions

By FRÉDÉRIC DIAS
Department of Ocean Engineering, Woods Hole Oceanographic Institution, Woods Hole, MA 02543, USA

ALAN R. ELCRAT
Department of Mathematics, Wichita State University, Wichita, KS 67208, USA

AND LLOYD N. TREFETHEN
Department of Mathematics, Massachusetts Institute of Technology, Cambridge, MA 02139, USA

(Received 5 January 1987 and in revised form 22 May 1987)

A jet is a stream of one fluid entering another at high speed. In the simplest classical model of jet flow, the geometry is two-dimensional, gravity and viscosity are ignored, the moving fluid is a liquid, and the stationary fluid is a gas whose influence is assumed negligible. The description of this idealized flow can be reduced to a problem of complex analysis, but, except for very simple nozzle geometries, that problem cannot be solved analytically. This paper presents an efficient procedure for solving the jet problem numerically in the case of an arbitrary polygonal nozzle.

## 1. Introduction

The study of liquid jets issuing from containers is centuries old. One classical result is Borda's 1766 prediction of the contraction coefficient $\frac{1}{2}$ for the case of a cylindrical orifice. In 1868, Helmholtz and Kirchhoff introduced the theory of free streamlines for such problems, together with the technique of solving them in two dimensions by complex analysis, and Helmholtz rederived the number $\frac{1}{2}$ by this new approach (Helmholtz 1868). The following decades saw extensions of the complex analysis methods by Planck, Joukowsky, Réthy, Levi-Civita, Greenhill, and others, culminating in a notable survey by von Mises (1917). Some substantial post-war compendia of this material are those of Birkhoff & Zarantonello (1957), Gilbarg (1960), Gurevich (1965), and Monakhov (1983), all of whom emphasize the close relationship of the mathematics of jets to that of cavities and wakes.

The classical theory of jets is elegant, but it has major limitations. Physically, it omits gravity, three-dimensionality, viscosity, and surface tension, and when such effects are introduced into the theory, the methods of complex analysis become harder to exploit. Mathematically, even in the idealized situation where complex analysis is fully applicable, only a few simple geometries can be treated in closed form. The reason is that the solution is related to a conformal map of Schwarz–Christoffel type that is impossible to determine analytically unless the container contains just two or three corners, or perhaps four or five if there is a line of symmetry. Consequently, few new geometries have been added to the collection of solved problems since von Mises.

The purpose of this paper is to address this mathematical limitation by describing an efficient numerical procedure for computing two-dimensional ideal jets issuing

from arbitrary polygonal containers. This procedure has enabled us to reproduce most of the flows in the above works by entering an appropriate sequence of vertices into the computer, and to explore new geometries interactively by drawing the boundary polygon with a mouse. Our computations are based upon numerical techniques developed earlier for Schwarz–Christoffel mapping (Trefethen 1980, 1983), but a modified Schwarz–Christoffel integral is required here because the free streamlines are not straight. In Elcrat & Trefethen (1986) a similar modified Schwarz–Christoffel procedure was described for wake and cavity flows.

Our methods can handle a container bounded by ten or fifteen vertices routinely in a few seconds of computer time. High accuracy is cheap: the amount of work is roughly proportional to the number of digits desired. Of course, it is rare that a 14-digit solution will match experiments any better than a 2-digit solution. The point is that if the classical model can be treated as solved, then one can concentrate on the physics.

With a certain amount of additional effort, Schwarz–Christoffel techniques can be adapted to include the effects of gravity. The first author has carried out such calculations for determining weir flows (Vanden-Broeck & Keller 1987), and will report this work in a later paper.

The history of this project is that independently during 1986, both the first author (Dias 1986) and the second and third authors adapted the ideas of Elcrat & Trefethen (1986) to the jet problem, but our methods are too similar for it to be appropriate to write two papers. Consequently, we have two independent Fortran programs, which can be obtained by contacting Dias or Trefethen. Dias's program is restricted to nozzles with parallel sides at infinity, as in Monakhov (1983). Those of our numerical results that satisfy this restriction have been checked by both programs.

## 2. Formulation of the problem

The geometry of our problem is shown in figure 1. An ideal incompressible fluid in the complex $z$-plane undergoes irrotational flow out of a reservoir bounded by two walls extending to infinity. The upper wall consists of a finite number of straight line segments delimited by finite vertices $z_1, \ldots, z_{L-1}$ and the infinite vertex $z_L = \infty$; the segment $(z_k, z_{k+1})$ is denoted by $\Gamma_k$. Similarly, the lower wall is delimited by $z_L$ and by finite vertices $z_{L+1}, \ldots, z_n$. The indices are ordered so that the flow region lies to the left as one traverses the boundary in the direction $z_1, \ldots, z_L, \ldots, z_n$.

Let $\gamma_k \pi$ denote the angle of $\Gamma_k$ counterclockwise from the real axis, defined up to a multiple of $2\pi$. For $k \leqslant L-1$ we think of $\Gamma_k$ as oriented in the direction $(z_{k+1}, z_k)$ to define $\gamma_k$, while for $k \geqslant L$ it is oriented in the direction $(z_k, z_{k+1})$. Let the external angle formed by $\Gamma_{k-1}$ and $\Gamma_k$ at the point $z_k$ be denoted by $\beta_k \pi = (\gamma_k - \gamma_{k-1})\pi$, plus a multiple of $2\pi$ if necessary to ensure that the following conditions hold. For each finite vertex, $\beta_k$ lies in the range

$$\text{finite vertex:} \quad -1 \leqslant \beta_k < 1, \quad k \neq L; \tag{1}$$

special cases of interest include a re-entrant slit ($\beta_k = -1$), a re-entrant right-angle corner ($\beta_k = -\frac{1}{2}$), a degenerate vertex at which there is no corner ($\beta_k = 0$), and a salient right-angle corner ($\beta_k = \frac{1}{2}$). At the infinite vertex $z_L$, $\beta_L$ lies in the range

$$\text{vertex at } \infty: \quad 0 \leqslant \beta_L \leqslant 2; \tag{2}$$

three special cases are a parallel channel at infinity ($\beta_L = 0$), a half-plane ($\beta_L = 1$), and the exterior of a parallel channel ($\beta_L = 2$). For non-integral values of $\beta_L$ in the

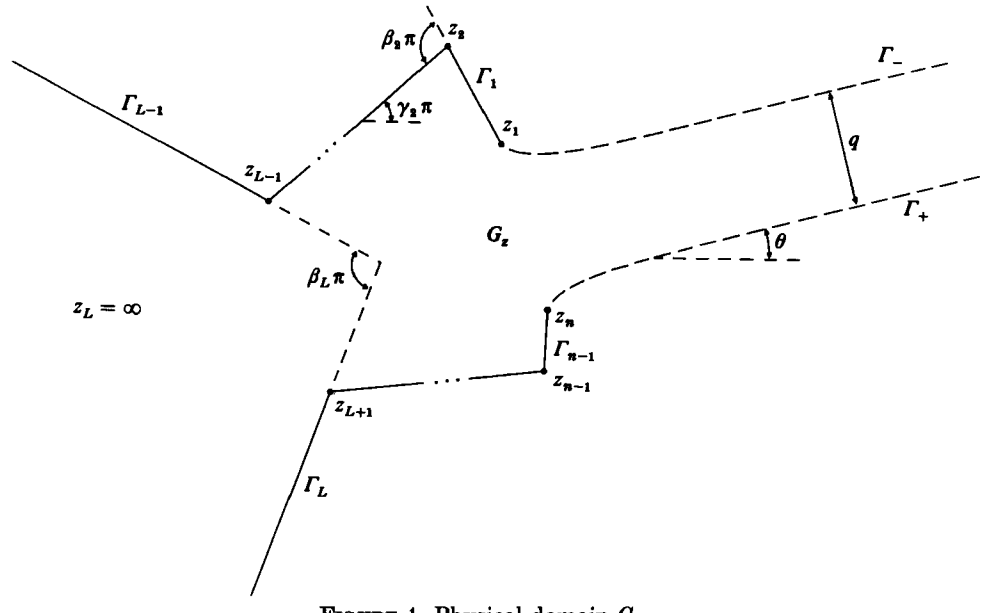


FIGURE 1. Physical domain $G_z$.

range (2), as illustrated in the figure, $\beta_L\pi$ is equal to the angle formed by extending the rays $\Gamma_{L-1}$ and $\Gamma_L$ to a finite intersection point.

Mathematically, it makes sense to permit arbitrary $\beta_k \in (-\infty, 1)$ for $k \neq L$ and $\beta_L \in (0, \infty)$. The resulting flows have physical meaning locally, but they cannot be imbedded in a plane, so their practical importance is limited.

Here is our problem of fluid mechanics: determine a potential flow $v(z)$ through the nozzle that continues to $z = \infty$ as a jet bounded by two free streamlines $\Gamma_-$ and $\Gamma_+$ on which the speed of flow is constant:

$$|v(z)| = 1 \quad \text{for} \quad z \in \Gamma_\pm. \tag{3}$$

This condition comes from Bernoulli's equation: a steady jet will have constant pressure $p = p_{\text{ambient}}$ on its bounding streamlines, and in the absence of gravity, this implies that $|v|$ is constant there. The shapes of the free streamlines are unknown *a priori*, and must be determined as part of the solution. Two other physical quantities to be determined are $\theta$, the angle of the jet at infinity, and $q$, the discharge rate. Because of the normalization (3), $q$ is equal to the width of the jet at infinity.

The flow problem can be reduced to a problem in complex analysis, as follows. Let $G_z$ denote the flow region bounded by the solid segments $\Gamma_k$ and the free streamlines $\Gamma_\pm$. Since the flow in $G_z$ is irrotational and incompressible, $v(z)$ is the gradient of a real velocity potential $\phi(z)$ defined in $G_z$ that satisfies $\nabla^2\phi = 0$. Let $v(z)$ be thought of as a complex scalar, and let $\zeta$ be its complex conjugate, the hodograph variable,

$$\zeta(z) = \bar{v}(z). \tag{4}$$

Then $\zeta$ is the complex derivative of a complex velocity potential $w(z) = \phi(z) + i\psi(z)$,

$$\zeta(z) = \frac{dw(z)}{dz}, \tag{5}$$

where the stream function $\psi$ is the harmonic conjugate of $\phi$. The function $w(z)$ is analytic in $G_z$, and maps $G_z$ conformally onto an infinite strip $G_w$ of height $q$, as shown

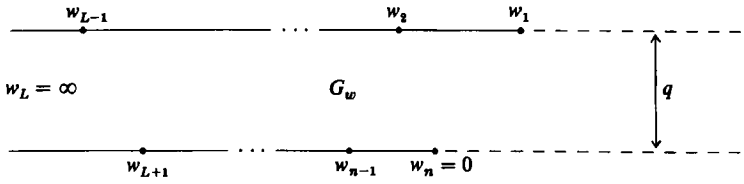


FIGURE 2. Velocity-potential domain $G_w$.

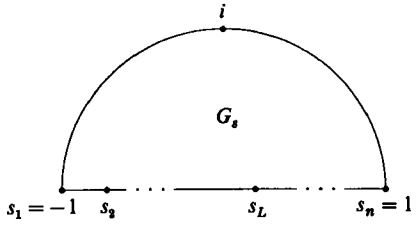


FIGURE 3. Computational domain $G_s$.

in figure 2. Without loss of generality we shall fix $w_n = 0$, where $w_k$ denotes $w(z_k)$. The point $w_1$ then lies at a location to be determined on the line $\operatorname{Im} w = q$.

It will be convenient to reduce $G_w$ to the upper half of the unit disk, with $w_1$ and $w_n$ corresponding to the points $-1$ and 1, respectively. First, a map of $G_w$ onto the upper half-plane is given by

$$\sigma = e^{\pi w/q}(1-\sigma_L)+\sigma_L, \quad w = \frac{q}{\pi}\log\left(\frac{\sigma-\sigma_L}{1-\sigma_L}\right), \tag{6}$$

with $\sigma_L$ chosen so that $\sigma(w_1) = -1$. (In Elcrat & Trefethen 1986 the half-plane was used for computations, but it is somewhat simpler to take one more step to the half-disk.) We then compose (6) with the mapping

$$s = \frac{1-(1-\sigma^2)^{\frac{1}{2}}}{\sigma}, \quad \sigma = \frac{2s}{1+s^2}. \tag{7}$$

The result is the following mapping between the infinite strip and the half-disk:

$$w = \frac{q}{\pi}\log\left(\frac{2s/(1+s^2)-2s_L/(1+s_L^2)}{1-2s_L/(1+s_L^2)}\right), \quad s = \frac{1-(1-(e^{\pi w/q}(1-\sigma_L)+\sigma_L)^2)^{\frac{1}{2}}}{e^{\pi w/q}(1-\sigma_L)+\sigma_L}. \tag{8}$$

Let $G_s$ denote the half-disk, with $s_k = s(w_k)$ for $1 \leqslant j \leqslant n$, as shown in figure 3. The points $s_k$ lie in the interval $[-1, 1]$. In the equations that follow we shall work with $s$ or $w$ interchangeably, according to convenience, since each is directly reducible to the other.

The restatement of the jet problem as a problem of complex analysis goes as follows. Our goal is to find a complex analytic function $z(s)$ in $G_s$ such that $\arg dz/dw$ takes prescribed piecewise-constant values for $s \in [-1, 1]$, and $|dz/dw|$ takes the value 1 for $s$ on the upper-half unit circle. A formulation in terms of the absolute angles $\gamma_k$ is ambiguous, since they are defined only up to multiples of $2\pi$, but a precise formulation can be based on the angle differences $\beta_k$. We must find an analytic function $z(s)$ in $G_s$ that satisfies the following conditions:

$$\arg\frac{dz}{dw} = \gamma_{n-1}\pi \qquad \text{at } s = s_n, \tag{9a}$$

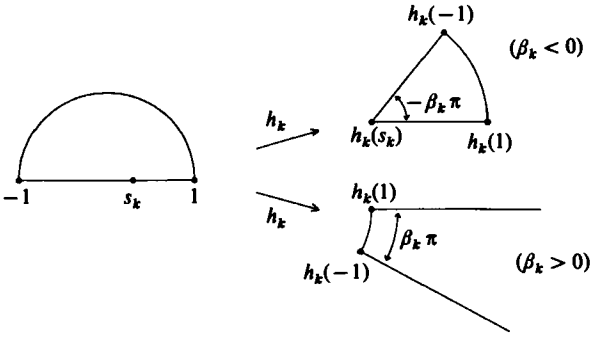


FIGURE 4. The factor $h_k$ in the modified Schwarz–Christoffel integral.

$$\Delta \arg \frac{\mathrm{d}z}{\mathrm{d}w} = \beta_k \pi \qquad \text{at } s = s_k, \quad 2 \leqslant k \leqslant n-1, \tag{9b}$$

$$\left|\frac{\mathrm{d}z}{\mathrm{d}w}\right| = 1 \qquad \text{for } |s| = 1, \quad \operatorname{Im} s \geqslant 0, \tag{9c}$$

$$|z(s_{k+1}) - z(s_k)| = |z_{k+1} - z_k|, \quad 1 \leqslant k \leqslant L-2, \quad L+1 \leqslant k \leqslant n-1, \tag{9d}$$

$$z(s_1) - z(s_n) = z_1 - z_n. \tag{9e}$$

The classical approach to determining $z(s)$ is to make use of the hodograph domain $G_\zeta$, which is the region in the $\zeta$-plane corresponding to $G_z$. $G_\zeta$ is bounded by radial lines and circular arcs, which become horizontal and vertical lines under a complex logarithm. Therefore, a disk or a half-plane can be mapped onto $\log(G_\zeta)$ by a Schwarz–Christoffel transformation. However, except for the simplest nozzle geometries, $\log(G_\zeta)$ turns out to be not a planar polygon but a polygonal Riemann surface, with a boundary topology that is not fully determined *a priori*, and the required Schwarz–Christoffel map is of a generalized kind whose determination is not straightforward. We will circumvent all of these problems by working with the mapping from $G_s$ to $G_z$. This also obviates the need for an additional numerical integration of (5).

The Schwarz–Christoffel transformation maps a half-plane onto a polygon or, in other words, it provides an analytic function whose derivative has a prescribed piecewise-constant argument. Equations (9) represent a modification of this standard situation that can be solved by a modified Schwarz–Christoffel formula (Elcrat & Trefethen 1986). Let $h_k(s)$ be defined by

$$h_k(s) = \left(\frac{s - s_k}{1 - s_k s}\right)^{-\beta_k}, \tag{10}$$

with the branch chosen so that $h_k(s) > 0$ for $s \in (s_k, 1)$. Then $h_k$ maps $G_s$ onto a pie slice (if $\beta_k < 0$) or the complement of a pie slice (if $\beta_k > 0$), as illustrated in figure 4. For an explicit representation of the function $\mathrm{d}z/\mathrm{d}w$ of (9), we can simply take a product of factors $h_k$:

$$\frac{\mathrm{d}z}{\mathrm{d}w} = \mathrm{e}^{\mathrm{i}\gamma_{n-1}\pi} \prod_{k=2}^{n-1} \left(\frac{s - s_k}{1 - s_k s}\right)^{-\beta_k}. \tag{11}$$

By construction, this formula satisfies the argument conditions (9*a*, *b*), and it satisfies the magnitude condition (9*c*) too since each factor satisfies (9*c*) individually.

Integration gives a modified Schwarz–Christoffel formula for the map from $G_s$ to $G_z$,

$$z(s_b)-z(s_a) = e^{i\gamma_{n-1}\pi}\int_{w_a}^{w_b}\prod_{k=2}^{n-1}\left(\frac{s-s_k}{1-s_k s}\right)^{-\beta_k} dw. \tag{12}$$

For this formula to be most useful we want to integrate with respect to $s$ rather than $w$. By (8), $dw$ can be replaced by

$$dw = \frac{dw}{ds}\,ds = \frac{q}{\pi}\frac{(1+s_L^2)(1-s^2)}{(1+s^2)(s-s_L)(1-s_L s)}\,ds,$$

and (12) becomes

$$z(s_b)-z(s_a) = \frac{q}{\pi}(1+s_L^2)\,e^{i\gamma_{n-1}\pi}\int_{s_a}^{s_b}\frac{1-s^2}{(1+s^2)(s-s_L)(1-s_L s)}\prod_{k=2}^{n-1}\left(\frac{s-s_k}{1-s_k s}\right)^{-\beta_k} ds. \tag{13}$$

Compare Monakhov (1983, p. 216).

This completes the mathematical formulation of our jet problem. We are still left with the task of satisfying the geometric conditions (9*d*, *e*). To accomplish this we will have to adjust $q$ and $s_2,\dots,s_{n-1}$ appropriately, and that is a matter for numerical computation.

## 3. Numerical procedure

The function (13) depends upon $n-1$ real parameters: $s_2,\dots,s_{n-1}$ and $q$. Correspondingly, it must satisfy $n-3$ real conditions (9*d*) and one complex condition (9*e*). Thus the count is right for the problem to have a unique solution (we shall not attempt a proof). The points $s_2,\dots,s_{n-1}$ are called accessory parameters or prevertices (since they are the preimages of the points $z_k$), and the problem of finding their correct values is the modified Schwarz–Christoffel parameter problem.

One of the unknowns can be eliminated by dividing each equation (9*d*) by the same equation (9*d*) with $k=1$. To carry this out mechanically, for any choice of $s_2,\dots,s_{n-1}$, let $q$ be arbitrary and compute $|z(s_2)-z(s_1)|$ by (13). (If $L=2$, we first introduce a degenerate vertex $z_2$ with $\beta_2=0$ and set $L=3$.) Now adjust $q$ so that the result becomes equal to $|z_2-z_1|$. What remains is a system of $n-2$ real nonlinear equations from (9*d*, *e*),

$$|z(s_{k+1})-z(s_k)|-|z_{k+1}-z_k| = 0, \quad 2\leqslant k\leqslant L-2, \quad L+1\leqslant k\leqslant n-1, \tag{14a}$$

$$z(s_1)-z(s_n)-(z_1-z_n) = 0, \tag{14b}$$

in $n-2$ real unknowns, $s_2,\dots,s_{n-1}$,

which must satisfy the constraints

$$-1 = s_1 < s_2 < \dots < s_{n-1} < s_n = 1. \tag{15}$$

We are thus faced with the problem of computing a numerical solution to a constrained nonlinear system of equations of size $n-2$. From this point the details are largely the same as in Elcrat & Trefethen (1986) concerning wakes and cavities. The essentials can be summarized as follows.

*Change of variables to eliminate constraints.* The constraints (15) are eliminated by the substitution

$$t_k = \log\frac{s_k-s_{k-1}}{s_{k+1}-s_k}, \quad s_{k+1} = s_k+(s_k-s_{k-1})\,e^{-t_k}, \quad 2\leqslant k\leqslant n-1. \tag{16}$$

The computer program works with the unconstrained variables $t_k$, converting from $t_k$ to $s_k$ whenever necessary.

*Solution of nonlinear system of equations.* The second and third authors have used the packaged code NS01A by Powell (1970) and the first author has used the packaged code ZXSSQ from the IMSL Library (IMSL 1986). Convergence is typically achieved with either program in on the order of $5(n-2)$ evaluations of the set of functions (14).

*Numerical integration.* The integral (13) must be evaluated numerically. A simple but effective approach used by the first author is to eliminate endpoint singularities with a change of variables, and then call an adaptive integrator such as DCADRE (IMSL 1986). A somewhat more efficient method (used by the second and third authors – 2–4 times faster) is compound Gauss–Jacobi quadrature, based on the subroutine GAUSSQ of Golub & Welsch (1969). 'Compound' quadrature refers to an adaptive aspect of the algorithm that is indispensable for accuracy: each interval of integration is automatically subdivided so as to ensure that no interval on which a Gaussian rule is applied is ever longer than the distance to the nearest singularity other than one of its endpoints. The singularities in question are $s = i$ and $s_k$ for $k = 1, \ldots, n$.

*Numerical integration near the separation points.* The integrand of (13) is analytic at $s_1$ and $s_n$ and has zeros there. (The reason is that near $s_1$ and $s_n$, $\mathrm{d}w/\mathrm{d}z$ maps one intersection of a straight line and a circle at right angles onto another such intersection; the proof can be completed by taking a logarithm and applying the reflection principle.) Therefore no special treatment of the integral near these points is required. The second and third authors have applied Gauss–Jacobi quadrature with linear weight functions to take advantage of the zeros of the integrand.

*Computation of $q$ and $\theta$.* The determination of a current estimate of the discharge rate $q$ is the first step of each iteration, as described above; when the process converges, $q$ will have the correct value. The angle $\theta$ of the jet at infinity is found by calculating the argument of (11) at $s = i$. The result is

$$\theta = \gamma_{n-1}\pi - \sum_{k=2}^{n-1} \beta_k(\tfrac{1}{2}\pi + 2\tan^{-1} s_k). \tag{17}$$

*Plotting flow lines.* The streamlines and equipotential lines in $G_z$ are the conformal images of a rectilinear grid in $G_w$, and to plot them, we compute the images $z(w)$ of a large number of points on the grid. Considerable time can be saved by making use of a subroutine to carry this out adaptively in such a way that the spacing between adjacent points $w$ is inversely related to the local curvature.

*Evaluation of the inverse map.* This is an easy job for Newton's method, which can take advantage of the fact that $\mathrm{d}z/\mathrm{d}s$ is equal to the integrand in (13). The inverse map is needed if one wants to determine the velocity at a specified point $z$, but not for computing $q$ and $\theta$ or plotting flow lines.

We have implemented the techniques described above in Fortran packages called FSFLOW (first author) and JET1 (second and third authors). Exclusive of comment cards and library software, the length of each package is about 250 lines, plus 150 more for driver commands and plotting. The amount of work involved in solving the parameter problem by JET1 can be very roughly estimated as

$$\text{Work} = 20D(n-2)^3 \text{ complex logarithms}, \tag{18}$$

where $D$ is the number of digits of accuracy required; we control the accuracy by taking $D$ quadrature points in each compound Gauss–Jacobi quadrature subinterval.

The time for FSFLOW is similar. The complex logarithm is a rather unusual work unit, but it is convenient for our problem because the exponentiation in (11), which is programmed by means of a complex logarithm, accounts for more than half of the total computation time. (This time can be cut in half by using real arithmetic in solving the parameter problem, since (14*a*) involves only absolute values, but complex logarithms are still required for subsequent plotting of the flow net.) For simple geometries on a Sun 3 workstation, the parameter problem is solved to 5-digit accuracy in 5–10 s, and plotting flow lines takes 1–10 times as long.

## 4. Computed examples

We began by duplicating a number of the cases considered in the literature. In the following examples $\theta$ is the angle of the jet at infinity, as in figure 1, and the aperture size $|z_n - z_1|$ is equal to 1 except where otherwise indicated. This means that $q$ can be interpreted as a contraction coefficient. Each plot shows streamlines separated by $\frac{1}{10}q$ and equipotential lines separated by $\frac{1}{5}q$. Notice that the spacing along the free streamlines in each plot is uniform, confirming that the constant-speed condition (3) has been satisfied.

*Symmetric funnel.* The simplest nozzle geometry is the symmetric funnel of half-angle $\alpha(=\frac{1}{2}\pi(\beta_L - 1))$. The contraction coefficient for general $\alpha$, first determined by von Mises, is given by

$$q^{-1} = 1 + \int_0^1 \operatorname{cotan} \tfrac{1}{2}\pi x \sin \alpha x \, dx$$

$$= 2 - \frac{1}{\pi} \sin \tfrac{1}{2}\pi \left[\psi(\tfrac{1}{2} + \tfrac{1}{2}\alpha) - \psi(\tfrac{1}{2}\alpha) - \alpha^{-1}\right], \tag{19}$$

where $\psi(x) = \Gamma'(x)/\Gamma(x)$ is the logarithmic derivative of the gamma function (Gilbarg 1960, p. 342; Gurevich 1965, p. 46). For $\alpha = 0°$, 45°, 90°, 135°, 180°, the contraction coefficients are $q = 1$, 0.7467, 0.6110, 0.5373, 0.5, respectively. (The number 0.7467 is usually reported incorrectly in the literature as 0.745 or 0.746.) Figures 5 and 6 show the textbook cases $\alpha = 180°$ (Borda, Helmholtz) and $\alpha = 90°$ (Kirchhoff, Rayleigh).

*Symmetric slot in pipe.* Figure 7 shows another symmetric flow, first calculated by Michell and Réthy, in which an aperture appears at the end of a channel of height $h$. The values $h = 1$ and $\infty$ correspond to the symmetric funnel with $\alpha = 0°$, 90°. For $h = 1$, 2, 5, 10, $\infty$, the numbers are $q = 1$, 0.6444, 0.6158, 0.6122, 0.6110.

*Asymmetric slot in pipe.* The flows become more interesting when we allow asymmetry. Figure 8 shows the same channel as before, but with the aperture adjacent to one boundary. For $h = 1$, 2, 5, 10, $\infty$, the contraction coefficients are $q = 1$, 0.7092, 0.6796, 0.6757, 0.6744, and the angles at $\infty$ are $-\theta = 0°$, 19.02°, 20.83°, 21.06°, 21.13°.

*Slot in side of pipe.* Analogously, figure 9 shows an aperture in the side of a pipe of height $h = 2$, located at a distance 1 from the end. For $h = 1$, 2, 5, 10, $\infty$ the contraction coefficients are $q = 0.5439$, 0.5926, 0.6093, 0.6120, 0.6129, and the jet angles are $-\theta = 74.21°$, 81.28°, 85.17°, 85.92°, 86.18°. If the aperture on the side is at the end of the pipe, these numbers become $q = 0.5780$, 0.6453, 0.6694, 0.6732, 0.6744 and $-\theta = 63.65°$, 67.19°, 68.58°, 68.79°, 68.87°.

*The 'teapot effect'.* The jets shown in the last few figures do not represent the only

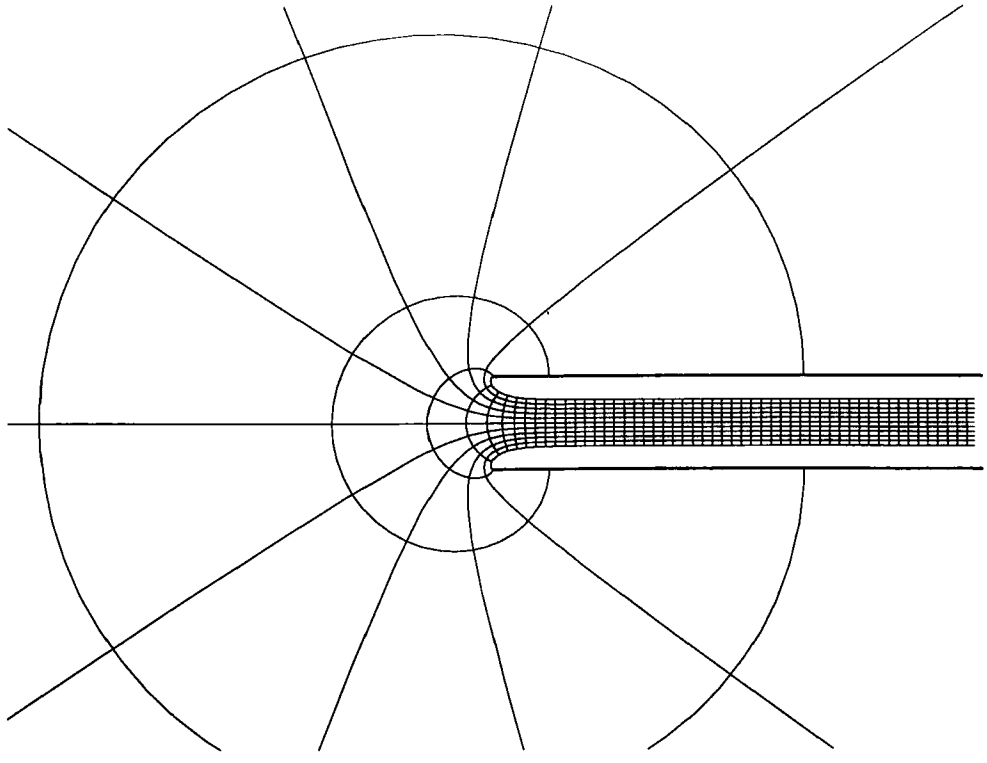

FIGURE 5. The Borda mouthpiece (symmetric funnel with $\alpha = 180°$).

free-streamline flows issuing from pipes. In a paper in 1957, J. B. Keller pointed out that additional solutions exist in which the fluid bends around the orifice to adhere to the outside of the pipe, and that solutions of this kind account for the tendency of some teapots to drip (Keller 1957). It would be a straightforward matter to modify the formulation described here to handle flows of this kind with a single free streamline, but instead, figure 10 shows the result of simulating such a geometry with our standard computer program based on a pair of free streamlines. The pipe has width 1, and the solid lower boundary actually bends back on itself for a distance $a = 6$ before giving way to a second free streamline (virtually straight), outside the range of the plot. In the limit $a \to \infty$ the jet has width $q = 2$ and angle $\theta = -180°$. For finite values $a = 1, 2, 4, 6$, the corresponding figures are $q = 1.9913$, 1.9989, 1.999964, 1.9999985, and $-\theta = 159.931°$, 172.837°, 178.702°, 179.737°.

*Finite Borda mouthpiece with lip.* Figure 11 shows the flow out of a finite-length Borda mouthpiece of width 1 and length $d = 1$. We have also added a divergent lip of length $\frac{1}{2}$ at angle 30°. For $d = 0$, 1, 2, 5, $\infty$, the values of $q$ are 0.7874, 0.7619, 0.7543, 0.7467, 0.7389, and the corresponding contraction coefficients are 0.5249, 0.5080, 0.5028, 0.4978, 0.4926. Note that contraction coefficients smaller than $\frac{1}{2}$ are possible. If the lip is removed, $q$ and the contraction coefficient become equal and take values 0.6110, 0.5129, 0.5076, 0.5035, 0.5000.

*Flow that crosses itself.* Nothing in our formulation prevents the flow from crossing itself in a non-physical fashion, as figure 12 shows by a simple example. The finite boundary segments have length 1, and the aperture has width 2. The value of $q$ (twice

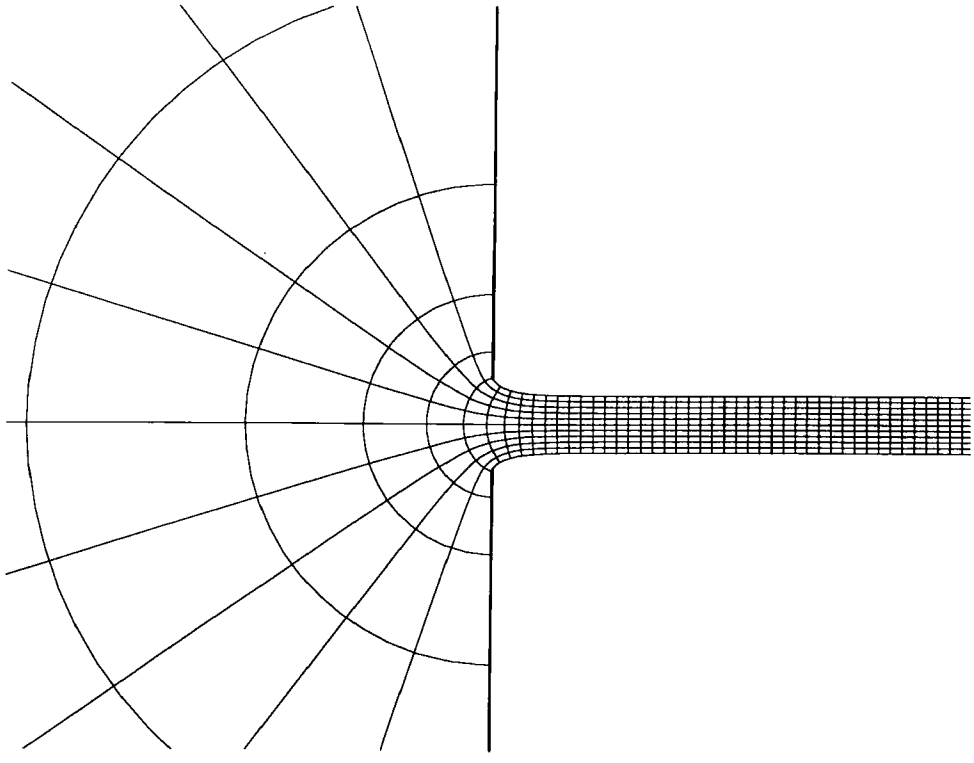

FIGURE 6. Slot in a plate (symmetric funnel with $\alpha = 90°$).

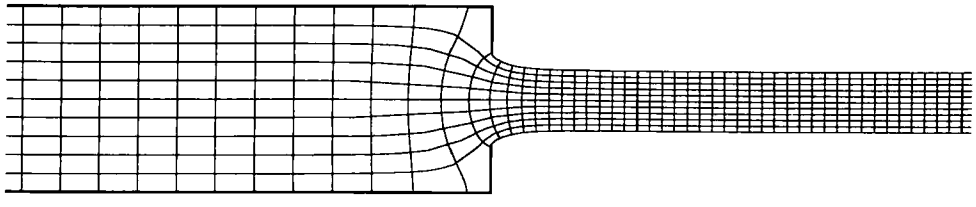

FIGURE 7. Symmetric pipe of height 2, aperture 1.

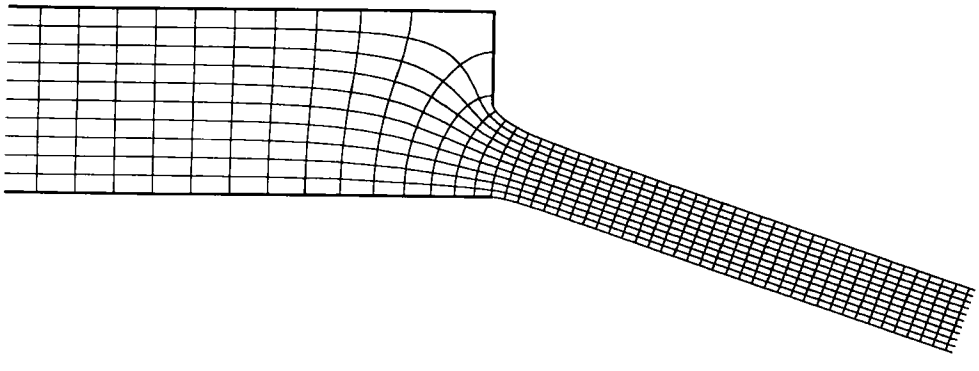

FIGURE 8. Asymmetric pipe of height 2, aperture 1.

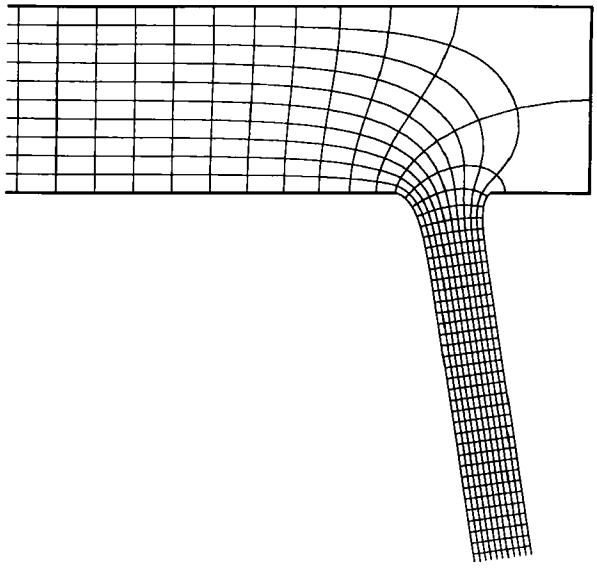

FIGURE 9. Aperture of length 1 in side of pipe of height 2.

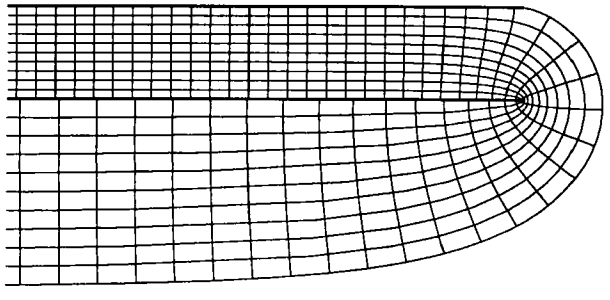

FIGURE 10. The 'teapot effect' – pouring flow out of a pipe of width 1.

the contraction coefficient) is 0.5797, and the jet angle is $\theta = 69.28°$. To determine a flow for this geometry in which the jet did not pass through the solid boundary, one would have to modify the mathematical model.

*Mouthpiece with circular lip.* Figure 13 shows a reservoir bounded by a horizontal boundary extending to $z = -i$ and then curving upwards in a quarter-circular arc to $z = 1$. The upper boundary is a straight line at angle 22.5° that begins at $z = -1$. Our Schwarz–Christoffel formulation of the jet problem cannot treat curved boundaries explicitly, so in the figure the quarter-circle has been approximated by $m = 16$ line segments. For $m = 1, 2, 4, 8, 16$, the computed values of $q$ (twice the contraction coefficient) are 0.7431, 0.7582, 0.7593, 0.7590, 0.7587, and the jet angles are $\theta =$ 41.24°, 52.83°, 56.38°, 57.56°, 57.97°. Evidently the convergence to limiting values as $m \to \infty$ is slow. We do not recommend the approximation of curved boundaries by polygons as a general procedure for, as (19) indicates, such an approach is very expensive. Just as in numerical conformal mapping (Trefethen 1986), methods designed expressly for curved boundaries should be used instead.

*A complicated example.* Finally, figure 14 shows a more whimsical nozzle with $n = 16$. The four longer segments near the aperture have horizontal displacement 1

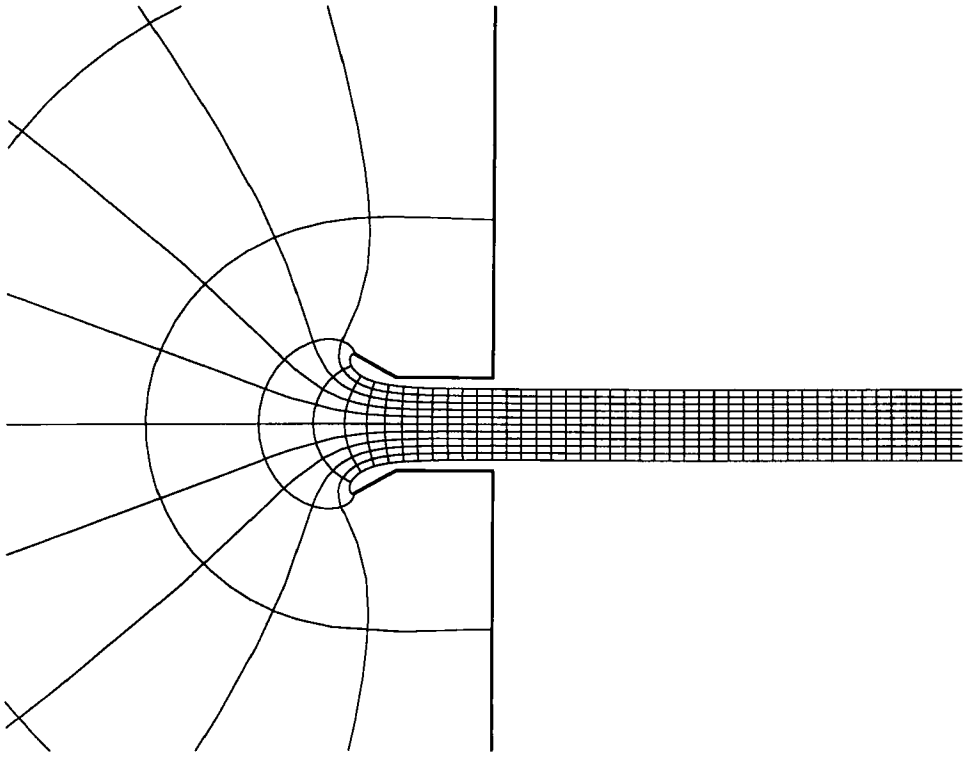

FIGURE 11. Finite Borda mouthpiece with divergent lip of length $\frac{1}{2}$, angle 30°.

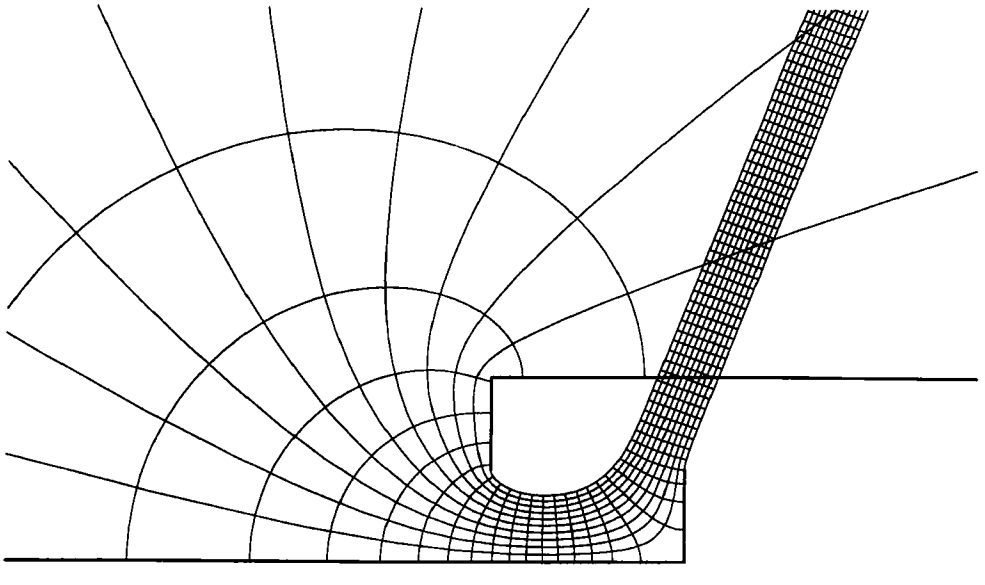

FIGURE 12. Non-physical flow that crosses itself.

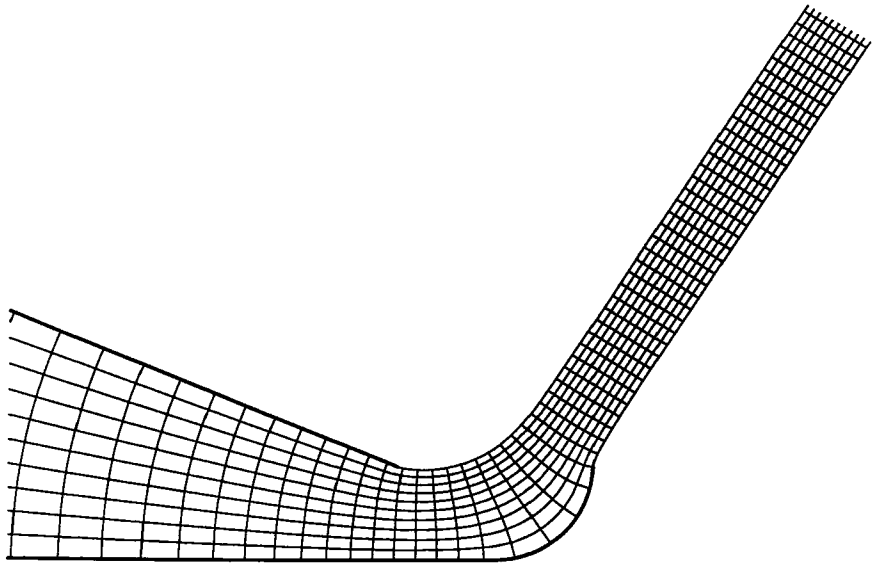

FIGURE 13. Mouthpiece with quarter-circular lip approximated by 16 line segments.

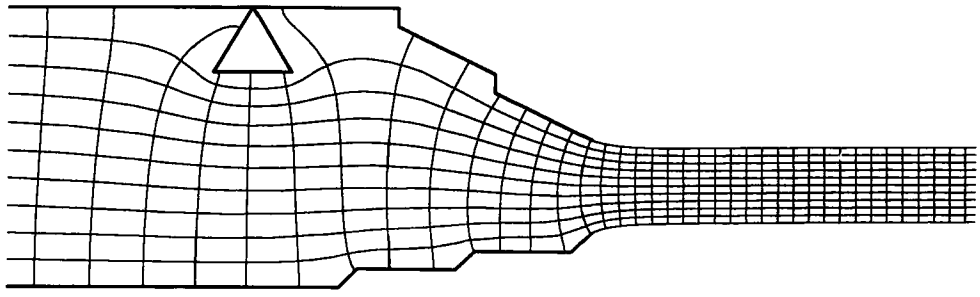

FIGURE 14. A more complicated example.

and vertical displacement 0 or 0.5. The four shorter segments have vertical displacement 0.2 and horizontal displacement 0 or 0.2. The aperture has height 1. The equilateral triangle, which is delimited by vertices $z_6$, $z_7$, $z_8$, and $z_9 = z_6$, has sides of length 0.8 and is located at a distance 1.5 from the corner to its right. The computed results for this problem are $q = 0.80090$ and $\theta = 0.455°$. If the triangular obstacle is removed, these figures change almost negligibly to $q = 0.80092$ and $\theta = 0.353°$.

A. R. E. was supported by US Air Force Grant AFOSR-86-0274, and L. N. T. by US Air Force Grant AFOSR-87-0102 and an IBM Faculty Development Award.

## REFERENCES

BIRKHOFF, G. & ZARANTONELLO, E. H. 1957 *Jets, Wakes, and Cavities*. Academic.

DIAS, F. L. 1986 *On the use of the Schwarz–Christoffel transformation for the numerical solution of potential flow problems*. Ph.D. dissertation, Dept. Civil and Env. Engng, University of Wisconsin-Madison.

ELCRAT, A. R. & TREFETHEN, L. N. 1986 Free-streamline flow over a polygonal obstacle. *J. Comp. Appl. Math.* **14**, 251–265. (Reprinted in Trefethen 1986.)

GILBARG, D. 1960 Jets and Cavities. *Handbuch der Physik*, vol. 9, 311–445.

GOLUB, G. H. & WELSCH, J. H. 1969 Calculation of Gaussian quadrature rules. *Math. Comput.* **23**, 221–230.

GUREVICH, M. I. 1965 *Theory of Jets in Ideal Fluids*. Academic.

HELMHOLTZ, H. 1868 On discontinuous movements of fluids. *Phil. Mag.* **36**, 337–346.

IMSL Inc 1986 The IMSL Library, 2500 Park West Tower One, 2500 City West Blvd., Houston, TX 77042-3020.

KELLER, J. B. 1957 Teapot effect. *J. Appl. Phys.* **28**, 859–864.

MISES, R. VON 1917 Berechnung von Ausfluss- und Überfallzahlen. *Zeit. des Vereines deutscher Ingenieure* **61**, 447–452, 469–474, 493–498. Reprinted in Frank, P. *et al.* eds., *Selected Papers of Richard von Mises*, Amer. Math. Soc., 1963.

MONAKHOV, V. N. 1983 *Boundary-value Problems with Free Boundaries for Elliptic Systems of Equations*. Trans. of Math. Monographs, vol. 57. Amer. Math. Soc.

POWELL, M. J. D. 1970 A Fortran subroutine for solving systems for nonlinear algebraic equations. In *Numerical Methods for Nonlinear Algebraic Equations* (ed. P. Rabinowitz). Gordon and Breach.

TREFETHEN, L. N. 1980 Numerical computation of the Schwarz–Christoffel transformation. *SIAM J. Sci. Stat. Comput.* **1**, 82–102.

TREFETHEN, L. N. 1983 SCPACK Version 2 User's Guide. *Int. Rep.* 24. Institute for Computer Applications in Science and Engineering, NASA Langley Research Center.

TREFETHEN, L. N., ed. 1986 *Numerical Conformal Mapping*. North-Holland.

VANDEN-BROECK, J.-M. & KELLER, J. B. 1987 Weir flows. *J. Fluid Mech.* **176**, 283–293.